

A BAYESIAN APPROACH TO THE VERTICAL STRUCTURE OF THE DISK OF THE MILKY WAY

DOBBIE P.^{1,2} AND WARREN S. J.²

¹Sydney, NSW, Australia. *phillip.dobbie@gmail.com* and

²Astrophysics Group, Blackett Laboratory, Imperial College London, London SW7 2AZ, UK

This work investigates the vertical profile of the stars in the disk of the Milky Way. The models investigated are of the form $\text{sech}^{2/n}(nz/(2H))$ where, setting $\alpha = 2/n$, the three functions of the sequence $\alpha = 0, 1, 2$ correspond to exponential, sech, sech^2 functions. We consider symmetric models and asymmetric models, above and below the plane. The study uses the large sample of K and M stars of Ferguson et al. (2017) and applies the methods of Bayesian model comparison to discriminate between the 6 models. Two inconsistencies in Ferguson et al. (2017), concerning the vertical height cut and the model continuity across the plane, are noted and addressed. We find that (1) in the Milky Way the symmetric disc models are decisively ruled out, with northern thin disc scale heights $\sim 25\%$ larger than southern, (2) there is moderate evidence for the exponential and sech models over the sech^2 model, though a sample extending further into the Galactic mid-plane is needed to strengthen this result, (3) the photometric distances used by Ferguson et al. (2017) underestimate the GAIA distances by a factor of roughly 1.16, and (4) the increase of scale height with Galactic latitude observed by Ferguson et al. (2017) is due to incorrect cuts to the data.

1. INTRODUCTION

The vertical profile of the density of stars in the disk of the Milky Way has been the subject of numerous studies. Over a limited range of heights z from the plane, the density variation may be modelled as exponential $e^{-z/H}$, where H is a scale height. Close to the plane the density profile is assumed to soften, and a functional form $\text{sech}^2(z/(2H))$ is commonly employed. The sech^2 function asymptotes to the exponential function for $z \gg H$. Beyond a few scale heights there is an excess in the tail, requiring a second population, of larger scale height. The two populations are the thin and the thick disk (Gilmore and Reid 1983). Fitting two populations provides a useful approximation to the structure of the disk, but this is itself a simplification (e.g. Bovy et al. 2012; Xiang et al. 2018).

The sech^2 and exponential functions are specific examples of a family of models of the form $\text{sech}^{2/n}(nz/(2H))$ (Van der Kruit 1988), where $n = 1$ is sech^2 and $n = \infty$ is exponential. In the following we use instead $\alpha = 2/n$, and consider the three functions of the sequence $\alpha = 0, 1, 2$, i.e. the exponential, sech, sech^2 functions. This is a sequence of successive flattening in the central plane. Matching sech^α to the exponential at large distances, the central-plane density is lower by the factor 2^α . In summary, eqs. (1) to (3) are possible parameterisations of the vertical variation of the stellar density as a function of vertical distance from the plane of the Milky Way:

$$n(z) = N_0 \left[e^{-\frac{|z+z_0|}{H_1}} + f e^{-\frac{|z+z_0|}{H_2}} \right] \quad (1)$$

$$n(z) = N_0 \left[\text{sech} \left(\frac{z+z_0}{H_1} \right) + f \text{sech} \left(\frac{z+z_0}{H_2} \right) \right] \quad (2)$$

$$n(z) = N_0 \left[\text{sech}^2 \left(\frac{z+z_0}{2H_1} \right) + f \text{sech}^2 \left(\frac{z+z_0}{2H_2} \right) \right] \quad (3)$$

The parameter z is now the height from the Sun and z_0 is the height of the Sun above the plane. The parameter f quantifies the density of the thick disk in the plane, relative to the density of the thin disk. The density in the midplane is $N_0(1+f)$.

The parameter α is of theoretical interest. The case $\alpha = 2$ corresponds to the equilibrium distribution of a uniform planar isothermal population of stars (Spitzer 1942), and is therefore a useful benchmark. The actual value of α is affected by the potential of the thinner gaseous disk, and is predicted to be smaller than the isothermal value at the solar radius (Banerjee and Jog 2007; Sarkar and Jog 2018).

There have been several measurements of α in external edge-on spiral galaxies. These are best undertaken in the K band to minimise the effects of extinction. The most detailed study of this topic is the analysis of de Grijs et al. (1997). For a sample of 24 galaxies they measure a distribution of values of $\alpha = 0.5 \pm 0.2$ (corrected for seeing and extinction), and argue that the true value is even lower, due to a bias because the galaxies are not perfectly edge on.

Most surveys used to analyse the structure of the Milky Way disk sample a conical volume centred on the Sun. Because of this the volume surveyed near the Galactic plane is too small to establish the density (and therefore the flattening) accurately there. Consequently there have been very few attempts to measure α for the Milky Way, and many authors simply assume $\alpha = 2$. There are no Milky Way studies for which the measurement of α was a primary aim. Among the studies of this question, Hammersley et al. (1999) state that ‘‘Analysis of one relatively isolated cut through an arm near longitude 65 degrees categorically precludes any possibility of a sech^2 stellar density function for the disc.’’ In contrast, using

GAIA DR1, Bovy (2017) states that for A to K stars “All vertical profiles are well represented by sech^2 profiles”. The selection function for this study is complicated, and he does not test other values of α . In addition, later than spectral type F the fits are not compelling.

The analysis of main-sequence turnoff and subgiant stars by Xiang et al. (2018), divided into bins of different age, provides the most detailed picture of the vertical structure of the disk in the solar neighbourhood (their Fig. 18). The measurement of α is a by-product of their study of the midplane stellar mass density. The survey selection function for this study is extremely complicated. Nevertheless the analysis demonstrates that α decreases with age, and for the whole sample (all ages combined) $\alpha \sim 0$, in disagreement with Bovy (2017).

A recent development in the measurement of the structure of the Milky Way disk has been the recognition that the stars are not in statistical equilibrium. Widrow et al. (2012) were the first to present evidence for a wave-like north-south asymmetry in the vertical number counts. This was subsequently confirmed in the more detailed studies of Yanny and Gardner (2013), Ferguson et al. (2017), and Bennett and Bovy (2019). The analysis of Ferguson et al. (2017) uses a very large sample of several million K and M stars, with photometric parallaxes, in matching footprints above and below the Galactic plane. This allows them to compare measurements of the scale heights above and below the plane, to quantify the asymmetry. They also investigated the shape of the number density distribution for different latitude ranges with a fixed range in longitude and found the scale heights to be sensitive to the selected latitude window. They invoked the different metallicities of the thin and thick disks (leading to errors in the photometric parallaxes) as a possible explanation for this effect.

The starting point for the current study was our interest in exploring whether the large sample of Ferguson et al. (2017) might provide an improved measurement of α for the Milky Way, and the possibility that the application of Bayesian model comparison techniques (e.g. Trotta 2008), which have been little used in this field, might lead to new insights. Early on we identified two inconsistencies in the analysis presented by Ferguson et al. (2017), and we explore the consequences here. The first of these is to do with the vertical height cut used in their analysis; this is explained in the next section. The second inconsistency is that in considering asymmetric models, in fitting independent scale heights both above and below the Galactic plane, there was no requirement imposed that the densities of the two functions match at the mid-plane. In our own analysis we impose continuity of density through the plane.

In the current paper we fit six different parametric models for the vertical density distribution to data from eight of the matched fields from Ferguson et al. (2017), correcting for the inconsistencies referred to above. We employ three values of $\alpha = 0, 1, 2$, eqs. (1) to (3), and we compare symmetric models (the same scale heights above and below the plane) against asymmetric models (different scale heights above and below the plane). We use a Bayesian approach for parameter estimation and model comparison. The aims are to determine whether an asymmetric model is required by the data, and to find

Field	b_1	b_2	l_1	l_2
1	30.0	55.1	55.0	60.0
2	32.8	59.3	60.0	65.0
3	37.2	65.3	70.0	75.0
4	48.6	72.8	95.0	105.0
5	49.0	73.4	105.0	120.0
6	48.7	73.6	120.0	135.0
7	46.7	71.7	135.0	150.0
8	51.0	68.5	150.0	165.0

TABLE 1
THE LATITUDE (B) AND LONGITUDE (L) LIMITS FOR THE EIGHT DATA SLICES INVESTIGATED; $b_1 < |b| < b_2$ AND $l_1 < l < l_2$.

if any values of α are ruled out. In Section 2 we describe the data set used, and the Bayesian formalism. In Section 3 we present the results in terms of the Bayesian evidence for the different models. Section 4 summarises.

2. METHODS

2.1. Data Selection

This study uses the sample of K and M stars selected by Ferguson et al. (2017) from the ninth data release of the Sloan Digital Sky Survey (SDSS). The complete dataset was kindly supplied to us by Sarah Gardner. Their sample selection built on the earlier works of Widrow et al. (2012) and Yanny and Gardner (2013). The selection was limited to fields above 30° in absolute Galactic latitude. The SDSS *gri* photometry was corrected for Galactic absorption, and limited to $15.0 < r_0 < 21.5$, and $1.8 < (g - i)_0 < 2.4$, where the subscript denotes values corrected for absorption. The distances to each star were computed using the photometric parallax relation provided by Ivezić et al. (2008), which relates absolute magnitude in the *r* band M_r to the $(g - i)_0$ colour, and includes a metallicity term. A fixed metallicity $[\text{Fe}/\text{H}] = -0.3$ was assumed. These distances were then refined using an additional small colour term determined by Yanny and Gardner (2013).

2.2. The Data Samples

The Ferguson et al. (2017) dataset comprises several subsamples. Each subsample covers an area matched above and below the Galactic plane, and is defined by limits in Galactic longitude l and absolute Galactic latitude $|b|$ (see their Fig. 3). There is one large matched data set, which we do not use, and a set of 14 smaller (individually) matched datasets. From these 14 we selected the 8 subsamples listed in Table 1 which cover a wide range in both l and b .

Ferguson et al. limit their analysis to the height range $0.35 \leq |z| \leq 2.0$ kpc, stating that the sample is complete in each field over the individual l and b ranges within the volume defined by these limits, and over the full range of colours $1.8 < (g - i)_0 < 2.4$. The justification that the sample is complete for all colours out to the upper limit comes from Yanny and Gardner (2013) (based on their Fig. 16). This argument is incorrect, as we now show.

In any direction on the sky there are lower and upper limiting distances, corresponding to the apparent magnitude range, that depend on colour. These limits are visible in the left-hand panel of Fig. 1, where the stars of one particular field are plotted. The sample is complete over all colours only within the distance range marked by

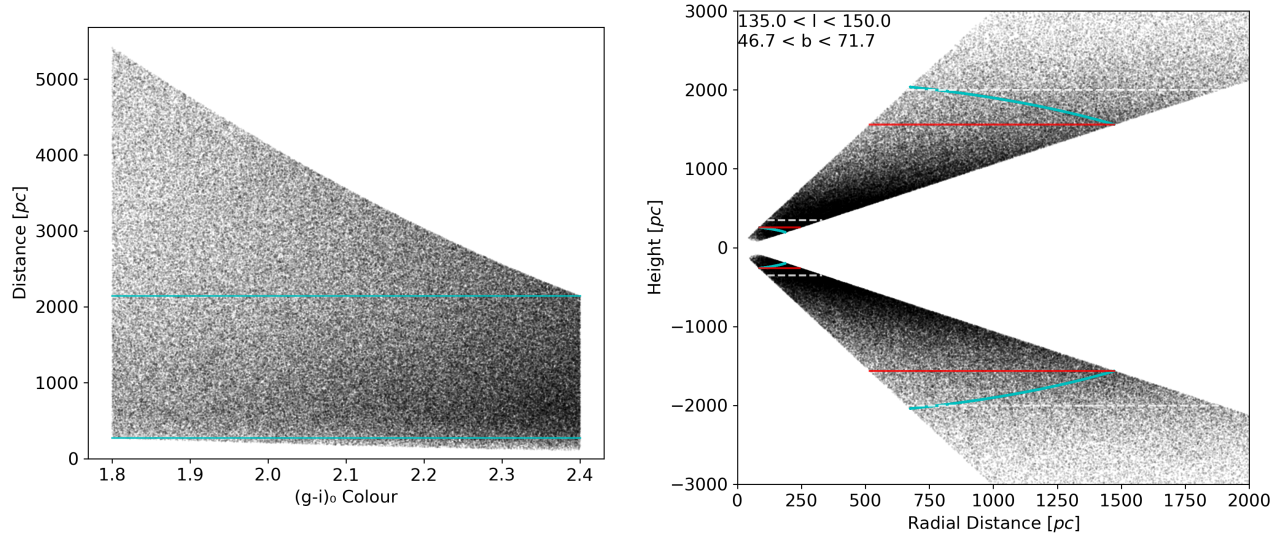


FIG. 1.— *LHS*: Plot of distance against colour for the subsample $135.0 < l < 150.0$ and $46.7 < |b| < 71.7$. The sample’s lower and upper distance limits correspond to the apparent magnitude limits $r_0 = 15.0$ and $r_0 = 21.5$ respectively. The sample is complete for all colours only over the distance range marked by the blue lines. *RHS*: The sample plotted in cylindrical coordinates z against cylindrical radius $r = \sqrt{x^2 + y^2}$. The blue lines are again the distance limits shown in the left-hand plot. The dashed white lines mark the z limits used by Ferguson et al. (2017). The red lines mark the z limits used in the current paper.

the blue lines i.e. between d_{min} for the bluest stars, hereafter $d_{min(blue)}$, and d_{max} for the reddest stars, hereafter $d_{max(red)}$. The same distance limits apply to all fields. These distance limits are shown in the polar plane, plotted in the right-hand panel. The z limits adopted by Ferguson et al. are shown by the dashed white lines.

Here it can be seen that horizontal slices are not complete over the full b range of the field for slices above the upper red line, which is lower than $z = 2$ kpc. The height of the red line, the correct upper completeness limit, is given by the expression $z_{lim(u)} = d_{max(red)} \sin(b_{min})$. The incompleteness introduced by adopting the wrong upper limit depends on the latitude range of the field, becoming more severe at lower latitudes. This might lead to visible trends with b , that are not real, of parameters of the measured Galactic structure. We return to this point in Section 3.3.

There is a corresponding lower completeness limit, also marked by a red line, given by the expression $z_{lim(l)} = d_{min(blue)} \sin(b_{max})$. Ferguson et al. (2017) adopt a lower height limit of 0.35 kpc. “due to brightness saturation effects”. However SDSS images are not saturated at $r = 15$, so we use instead $z_{lim(l)}$ as given above, which is smaller than 0.35 kpc in all fields. This is useful because probing closer to the Galactic plane improves the measurement of α .

The stellar number counts are divided into 50 bins, equally spaced in z between $z_{lim(l)}$ and $z_{lim(u)}$. The volume of a slice is

$$V(z) = \frac{1}{2} \delta (l_2 - l_1) z^2 \left(\frac{1}{\sin^2 b_1} - \frac{1}{\sin^2 b_2} \right) \quad (4)$$

where δ is the vertical thickness of the bin, z is the height of the middle point of the bin, and the ranges of longitude and latitude are $l_1 < l < l_2$ and $b_1 < |b| < b_2$. This is also the formula used by Ferguson et al. (2017). It would, of course, be possible to compute the space

density at heights greater than $z_{lim(u)}$ by selecting only sources within $d_{max(red)}$, with appropriate modification of the expression for the volume, but we chose not to, for simplicity.

2.3. Bayesian methodology

For parameter estimation and model comparison we use the PyMultiNest (Buchner et al. 2014) implementation of the MultiNest nested sampling algorithm (Feroz et al. 2009).

2.3.1. Parameter Estimation

For observed data D , background information I , and a model specified by a vector of parameters θ , Bayes’ theorem

$$\text{prob}(\theta|D, I) = \frac{\text{prob}(D|\theta, I) \text{prob}(\theta|I)}{\text{prob}(D|I)} \quad (5)$$

formulates the task of parameter estimation. The term on the left, the posterior, is the result sought, the probability of the parameters given the data. On the right, the first term in the numerator is the likelihood, which is the probability of the data given the parameters, and the second term is the prior for the parameters. The denominator is the Bayesian evidence, explained in Section 2.3.1, which is a normalisation constant that is not needed for parameter estimation.

Symmetric disk models, for each of the three model profiles, eqs. (1) to (3), are specified by five free parameters; N_0 , H_1 , H_2 , z_o , and f . We adopt broad uniform linear priors over the following ranges

$$\begin{aligned} 0.0 < N_0 < 10^9 \text{ kpc}^{-3} \\ 0.0 < H_1 < 2.0 \text{ kpc} \\ 0.0 < H_2 < 2.0 \text{ kpc} \\ 0.0 < z_o < 0.1 \text{ kpc} \\ 0.0 < f < 1.0 \end{aligned} \quad (6)$$

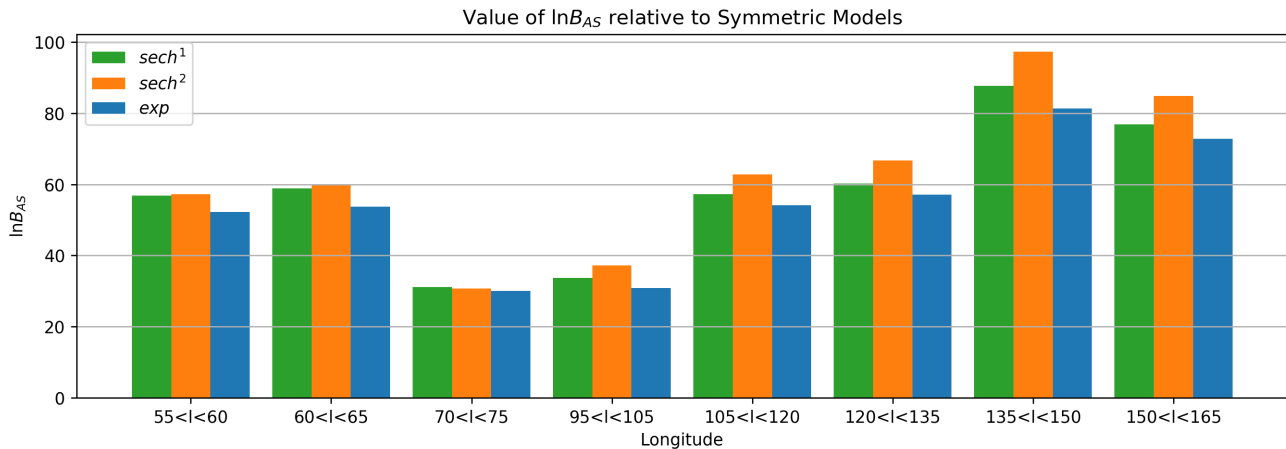


FIG. 2.— The $\ln B_{AS}$ values of the asymmetric models shown relative to the symmetric models for the same field.

For asymmetric models we must specify independent scale heights above (N) and below (S) the plane, H_{1N} , H_{2N} , H_{1S} , H_{2S} , meaning there are seven free parameters. The same broad uniform prior is used for all scale heights. In contrast to Ferguson et al. (2017), the density models above and below the plane share the same values of N_0 and f , ensuring that the density distribution is continuous through the disk mid-plane.

For any model, the likelihood is given by

$$\text{prob}(D|\theta, I) = \mathcal{L} = \prod_i \frac{1}{\sqrt{2\pi m_i}} e^{-\frac{(n_i - m_i)^2}{2m_i}} \quad (7)$$

Here n_i is the number of stars in slice i and m_i is the number of stars predicted by the model, and we have approximated the Poisson distribution by the Gaussian distribution since the number of stars in each slice is large. In practise the sampler uses the negative log likelihood (excluding a constant term)

$$-\ln \mathcal{L} = \sum \frac{(n_i - m_i)^2}{2m_i} + \frac{1}{2} \sum \ln m_i \quad (8)$$

Because the likelihood functions for these datasets are very narrow, the choice of priors does not significantly impact the estimation of parameters.

2.3.2. Model Comparison

Model comparison requires the calculation of the Bayesian evidence for each model, the denominator on the RHS of equation 5. The Bayesian evidence is the integral of the numerator over the parameter space i.e.

$$\text{prob}(D|M_i, I) = \int \text{prob}(D|\theta_i, M_i, I) \text{prob}(\theta_i|M_i, I) d\theta_i \quad (9)$$

where M_i specifies the model. Application of Bayes' theorem then leads to the following expression for the ratio of posteriors for two different models, M_1 , M_2 ,

$$\frac{\text{prob}(M_1|D, I)}{\text{prob}(M_2|D, I)} = \frac{\text{prob}(D|M_1, I) \text{prob}(M_1|I)}{\text{prob}(D|M_2, I) \text{prob}(M_2|I)} \quad (10)$$

Here $\text{prob}(M_i|I)$ is the prior for a model. We assume equal priors in all cases, in which case the problem re-

duces to computing the Bayes factor, given by

$$B_{12} = \frac{\text{prob}(D|M_1, I)}{\text{prob}(D|M_2, I)} \quad (11)$$

Trotta (2008) tabulates threshold values for considering a model to be superior, with $|\ln B_{12}| > 2.5$ listed as providing moderate evidence, and $|\ln B_{12}| > 5$ listed as providing strong evidence.

We argued above that the choice of priors does not impact the estimation of the parameters for the datasets used here. In comparing models, though, the priors are important. Although models with larger numbers of parameters will usually provide a better fit to the data, this is balanced in the calculation of the Bayesian evidence by the increased volume of parameter space over which the integral is performed. In comparing the symmetric models to the asymmetric models, the width of the priors for the extra scale heights then become important. This is because, for uniform priors over a width $H_{upper} - H_{lower}$, the probability density of the prior is inversely proportional to the width. This point must be borne in mind when considering the results, in the next section.

3. RESULTS AND DISCUSSION

In this study we are more interested in the comparison of different models than the values of the measured parameters. Three cases of α are considered, $\alpha = 0, 1, 2$, and we fit both symmetric and asymmetric models. These six models are each fit to the data from the eight fields listed in Table 1, providing 48 sets of results.

3.1. Comparison of symmetric and asymmetric models

We consider firstly the evidence for asymmetry in the density distribution, above and below the plane. We have measured the Bayes factor comparing the asymmetric model (A) to the symmetric model (S), B_{AS} , for each value of α , in each field, providing 24 values of B_{AS} . The values of $\ln(B_{AS})$ are plotted in Fig. 2. They range from 30 to 90. This is decisive evidence for the asymmetric model over the symmetric model. This is despite the rather broad priors used for all the scale heights $0 < H < 2$ kpc, which act to penalise the model with more parameters.

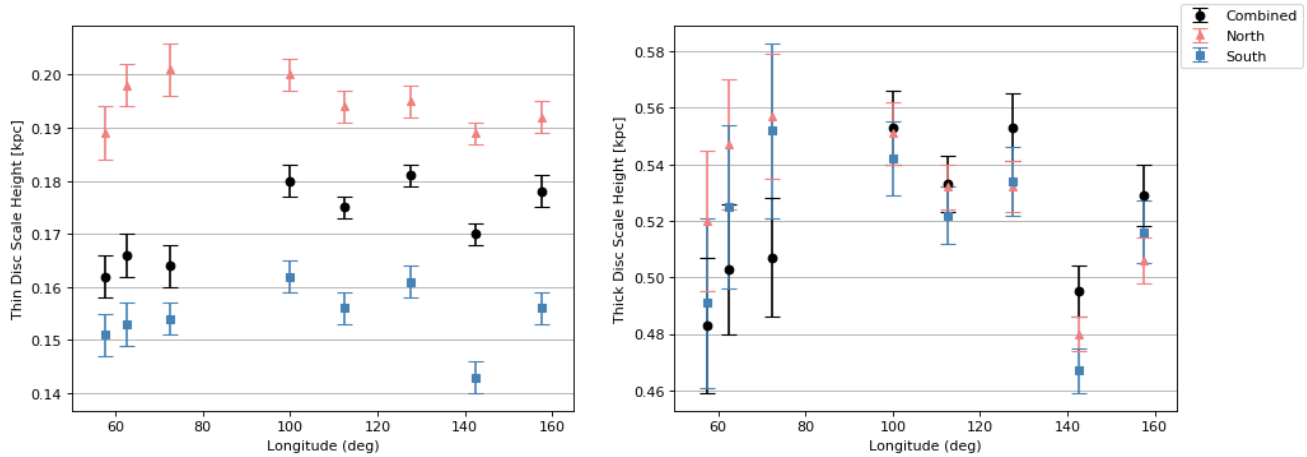


FIG. 3.— Scale height comparison for the sech^2 models. Thin disc scale heights shown in figure (a) and thick disc scale heights in figure (b). Circles represent the symmetric model, while triangles and squares are the North and South hemispheres of the asymmetric model respectively.

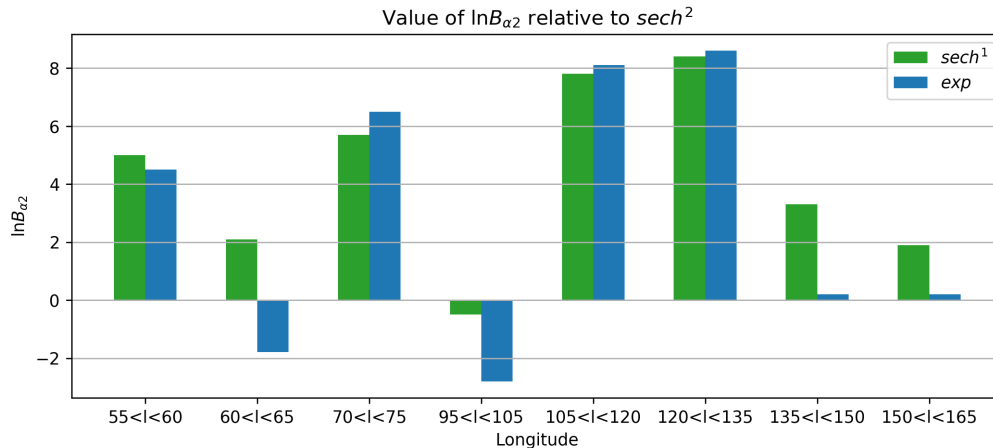


FIG. 4.— The $\ln B_{\alpha 2}$ values for exponential ($\alpha = 0$) and sech ($\alpha = 1$) models relative to sech^2 . The greater the value of $|\ln B_{\alpha 2}|$, the better suited the model is to the data relative to sech^2 .

The large values of B_{AS} are not particularly surprising, given that asymmetry in the density distribution is clearly visible in plots of the binned space density above and below the plane, e.g. figures in Ferguson et al. (2017). Nevertheless it is satisfying to see this so strongly confirmed by the Bayes factor analysis, and it suggests that model comparison could identify more subtle effects that might not be so readily apparent in the binned data.

The measured values of the respective scale heights for the thin and thick disks, for the symmetric and asymmetric models are plotted in Fig. 3, specifically for the $\alpha = 2$ models. For the thick disk (RHS) the scale heights above and below the plane are in good agreement. For the thin disk the scale heights above the plane are about 25% larger than the scale heights below the plane. The actual values measured are discussed below.

3.2. Comparison of different values of α

Because the asymmetric models are decisively preferred, in comparing the fits for different values of α we consider the asymmetric models only. In most cases the $\alpha = 2$ model i.e. sech^2 provides the worst fit. In Fig. 4

we plot the eight measured values of $\ln B_{02}$ and of $\ln B_{12}$ i.e. the values of the Bayes factors for the exponential and sech models relative to the sech^2 model. The average values of $\ln B_{02}$ and of $\ln B_{12}$ are 2.9 and 4.2 respectively. This is moderate evidence against the sech^2 model.

Examples of fits of the three different asymmetric models for two of the fields are provided in Fig. 5. In each field the three models appear very similar over the height ranges which are fit, i.e. where there is data, but the models are strikingly different at heights < 300 pc i.e. close to the plane where there is no data. In this respect it is impressive that the model comparison provides moderate evidence against the sech^2 model. It appears likely that applying the same model comparison method to a survey with data closer to the plane could definitively distinguish between the three different values of α .

The measured scale heights for a particular model are similar between different fields, as shown in Fig. 3. Typical values of the scale height for the thin disk are ~ 200 pc for the sech model, with slightly smaller (larger) values measured for the sech^2 (exponential) models. We mea-

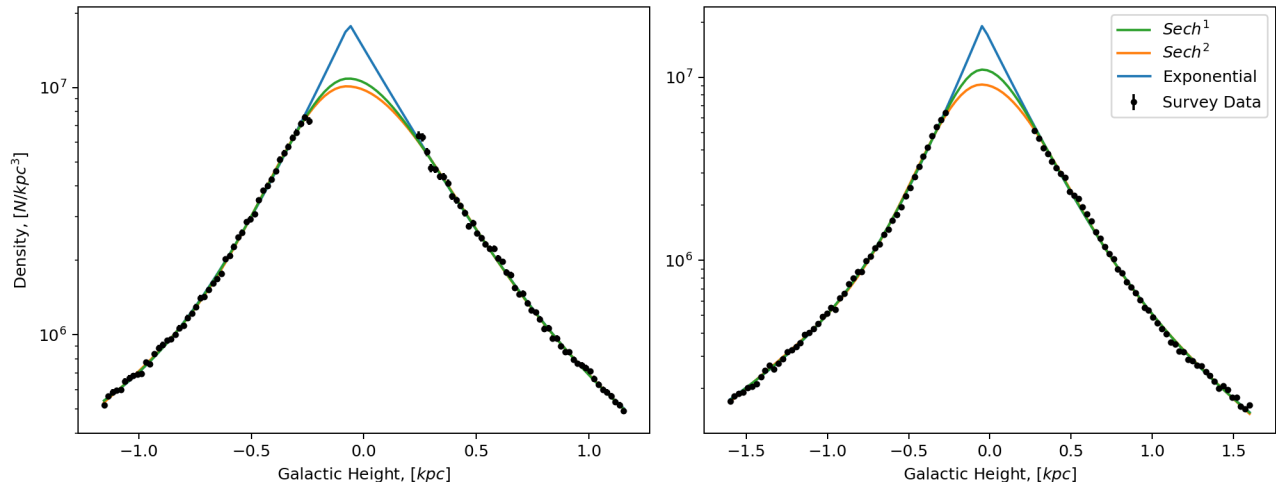


FIG. 5.— The three asymmetric model types plotted together for the data slices of $60 < l < 65$ (a) and $120 < l < 135$ (b) in log-space.

sure smaller scale heights than Ferguson et al. (2017). This statement applies even when we attempted to reproduce their results using the same cuts and fitting methods that they used, so it is not a consequence of these factors, and we have not found an explanation. Our measured scaleheight for the thin disk ~ 200 pc is noticeably smaller than the fiducial value of 300 pc (e.g. Bochanski et al. 2010; Gilmore and Reid 1983; Chang et al. 2011; Jurić et al. 2008). We have found that part of the discrepancy lies with the photometric parallaxes used by Ferguson et al. (2017). To check their distances we matched a subsample to the GAIA DR2 data release (Gaia Collaboration 2018). We started with all the sources in the N half of the field $48.7 < b < 73.6$, $120 < l < 135$, and selected sources matched within 1 arcsec, with $\text{parallax/error} > 30$, producing a sample of 5391 sources with accurate geometric parallaxes. We computed the ratio of the photometric distance over the geometric distance d_{ph}/d_{GAIA} . The median value of this ratio is 0.86 with a 1σ scatter of 0.12. This indicates that the photometric distances should be multiplied by a factor 1.16, implying a scale height of ~ 230 pc for the sech model.

A further correction needs to be made for the presence of binaries in the photometric sample. Applying this correction will act to increase the scale height (e.g. Covey et al. 2008; Bochanski et al. 2010). Alternatively we can compare against the scaleheight of 255 pc measured by Bochanski et al. (2010) which is the measured scaleheight before correction. These two numbers are now in reasonable agreement. In fact the correction for binaries will be somewhat larger for the sample of Ferguson et al. (2017) compared to that of Bochanski et al. (2010), because the stars are of earlier spectral type, on average, for which the binary fraction is larger (Duchêne and Kraus 2013). This means that the agreement is even better.

3.3. Trends with Galactic latitude

Ferguson et al. (2017) noted a trend between measured scale height and average Galactic latitude of each field measured, for both the thin and the thick disk. They

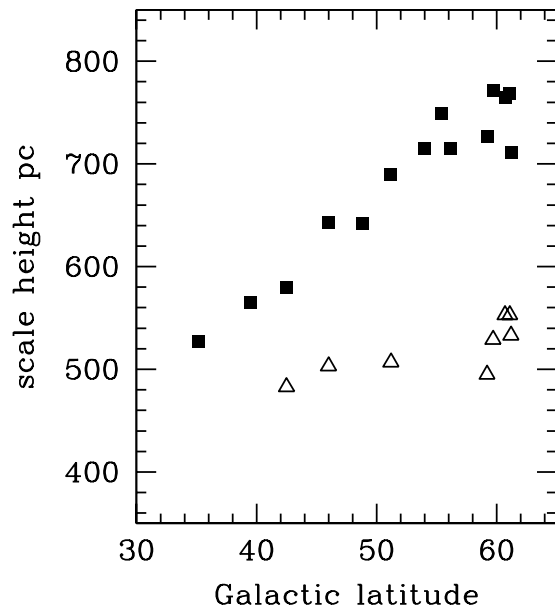


FIG. 6.— The scale height of the thick disk as a function of Galactic latitude b . Filled squares plot values from Ferguson et al. (2017), and open triangles plot values from this paper. In each case the data are for the symmetric sech^2 model.

ascribed this to metallicity trends that affect the distance estimates. In Fig 6 their measured scale heights for the thick disk are plotted, as filled squares, against average b for each field. These data are for the symmetric model and were extracted from their Fig. 7 (14 fields). There is a strong trend with b , and a similar trend is seen for their thin disk measurements. Our own measurements (8 fields) for the thick disk are plotted as open triangles, and do not display a strong trend with b . The same is true for our thin disk results. This indicates that the strong trend seen in the results of Ferguson et al. (2017) is an artifact caused by the incorrect distance cuts they applied, as anticipated in Section 2.2.

4. SUMMARY

We have used Bayesian model comparison to investigate the vertical structure of the disk of the Milky Way at the solar radius, using the large homogeneous sample of Ferguson et al. (2017). We corrected for two inconsistencies in the previous analysis by Ferguson et al. (2017), one to do with the completeness limits of the sample, and the other by ensuring that asymmetric density models above and below the plane are continuous through the mid plane. The main findings are:

1. Symmetric models for the vertical profile of the Galactic disk are decisively ruled out, based on the measured Bayes factors. The scale heights of the thin disk in the N are $\sim 25\%$ larger than in the S.

2. There is moderate evidence for the exponential or

sech models, respectively $\alpha = 0, 1$, over the sech² model, but a sample extending closer to the Galactic mid-plane is needed to strengthen this result.

3. The photometric distances used by Ferguson et al. (2017) underestimate the true distance by a factor 1.16 on average.

4. We have presented evidence that the strong trend of scale height with Galactic latitude b found by Ferguson et al. (2017) is due to incorrect cuts applied to the data.

After completing the calculations presented in this paper a new sample appeared which is highly suitable for analysis by the methods developed here (Ahmed and Warren 2019). The analysis of that sample will be presented in a forthcoming paper.

REFERENCES

- Ahmed, S., and Warren, S. (2019), “A homogeneous sample of 34 000 M7–M9.5 dwarfs brighter than $J=17.5$ with accurate spectral types,” *Astronomy & Astrophysics*, 623, A127.
- Banerjee, A., and Jog, C. J. (2007), “The Origin of Steep Vertical Stellar Distribution in the Galactic Disk,” *The Astrophysical Journal*, 662, 335–340.
- Bennett, M., and Bovy, J. (2019), “Vertical waves in the solar neighbourhood in Gaia DR2,” *MNRAS*, 482(1), 1417–1425.
- Bochanski, J. J., Hawley, S. L., Covey, K. R., West, A. A., Reid, I. N., Golimowski, D. A., and Ivezić, Z. (2010), “The Luminosity and Mass Functions of Low-mass Stars in the Galactic Disk. II. The Field,” *The Astronomical Journal*, 139(6), 2679–2699.
- Bovy, J. (2017), “Stellar Inventory of the Solar Neighborhood using Gaia DR1,” *Monthly Notices of the Royal Astronomical Society*, 470, 1360–1387.
- Bovy, J., Rix, H.-W., and Hogg, D. W. (2012), “The Milky Way Has No Distinct Thick Disk,” *The Astrophysical Journal*, 751, 131–137.
- Buchner, J., Georgakakis, A., Nandra, K., Hsu, L., Rangel, C., Brightman, M., Merloni, A., Salvato, M., Donley, J., and Kocevski, D. (2014), “X-ray spectral modelling of the AGN obscuring region in the CDFS: Bayesian model selection and catalogue,” *Astronomy & Astrophysics*, 564, A125.
- Chang, C.-K., Ko, C.-M., and Peng, T.-H. (2011), “Information on the Milky Way from the Two Micron All Sky Survey Whole Sky Star Count: The Structure Parameters,” *The Astrophysical Journal*, 740(1).
- Covey, K. R., Hawley, S. L., Bochanski, J. J., West, A. A., Reid, I. N., Golimowski, D. A., Davenport, J. R. A., Henry, T., Uomoto, A., and Holtzman, J. A. (2008), “The Luminosity and Mass Functions of Low-Mass Stars in the Galactic Disk. I. The Calibration Region,” *AJ*, 136(5), 1778–1798.
- de Grijs, R., Peletier, R., and van der Kruit, P. (1997), “The z-structure of disk galaxies towards galactic planes,” *Astronomy and Astrophysics*, 327, 966–982.
- Duchêne, G., and Kraus, A. (2013), “Stellar Multiplicity,” *ARA&A*, 51(1), 269–310.
- Ferguson, D., Gardner, S., and Yanny, B. (2017), “Milky Way Tomography with K and M Dwarf Stars: The Vertical Structure of the Galactic Disk,” *The Astrophysical Journal*, 843(2).
- Feroz, F., Hobson, M. P., and Bridges, M. (2009), “MULTINEST: an efficient and robust Bayesian inference tool for cosmology and particle physics,” *MNRAS*, 398(4), 1601–1614.
- Gaia Collaboration (2018), “Gaia Data Release 2. Summary of the contents and survey properties,” *A&A*, 616, A1.
- Gilmore, G., and Reid, N. (1983), “New light on faint stars. III - Galactic structure towards the South Pole and the Galactic thick disc,” *Monthly Notices of the Royal Astronomical Society*, 202(March), 1025–1047.
- Hammersley, P. L., Cohen, M., Garzón, F., Mahoney, T., and López-Corrodoira, M. (1999), “Structure in the first quadrant of the Galaxy: an analysis of TMGS star counts using the SKY model,” *MNRAS*, 308(2), 333–363.
- Ivezić, Ž., Sesar, B., Jurić, M., Bond, N., Dalcanton, J., Rockosi, C. M., Yanny, B., Newberg, H. J., Beers, T. C., Prieto, C. A. et al. (2008), “The milky way tomography with SDSS. II. Stellar metallicity,” *The Astrophysical Journal*, 684(1), 287.
- Jurić, M., Ivezić, Z., Brooks, A., Lupton, R. H., Schlegel, D., Finkbeiner, D., Padmanabhan, N., Bond, N., Sesar, B., Rockosi, C. M., Knapp, G. R., Gunn, J. E., Sumi, T., Schneider, D. P., Barentine, J. C., Brewington, H. J., Brinkmann, J., Fukugita, M., Harvanek, M., Kleinman, S. J., Krzesinski, J., Long, D., Neilsen, E. H. J., Nitta, A., Snedden, S. A., and York, D. G. (2008), “The Milky Way Tomography with SDSS. I. Stellar Number Density Distribution,” *The Astrophysical Journal*, 673(2), 864–914.
- Sarkar, S., and Jog, C. J. (2018), “The constraining effect of gas and the dark matter halo on the vertical stellar distribution of the Milky Way,” *A&A*, 617, A142.
- Spitzer, L. (1942), “The Dynamics of Interstellar Medium III. Galactic Distribution,” *The Astrophysical Journal*, 95(3), 329.
- Trotta, R. (2008), “Bayes in the sky: Bayesian inference and model selection in cosmology,” *Contemporary Physics*, 49(2), 71–104.
- Van der Kruit, P. (1988), “The three-dimensional distribution of light and mass in disks of spiral galaxies,” *Astronomy and Astrophysics*, 192(1-2), 117–127.
- Widrow, L. M., Gardner, S., Yanny, B., Dodelson, S., and Chen, H.-Y. (2012), “Galactoseismology: discovery of vertical waves in the Galactic Disk,” *The Astrophysical Journal Letters*, 750(2), L41.
- Xiang, M., Shi, J., Liu, X., Yuan, H., Chen, B., Huang, Y., Wang, C., Wu, Y., Tian, Z., Huo, Z., Zhang, H., and Zhang, M. (2018), “Stellar Mass Distribution and Star Formation History of the Galactic Disk Revealed by Mono-age Stellar Populations from LAMOST,” *ApJS*, 237(2), 33.
- Yanny, B., and Gardner, S. (2013), “The stellar number density distribution in the local solar neighborhood is North-South asymmetric,” *The Astrophysical Journal*, 777(2), 91.